AGU PUBLICATIONS

Geophysical Research Letters

RESEARCH LETTER
10.1002/2015GL065327

Key Points:
- The recent warming hiatus is strongly influenced by a pronounced Eurasian winter cooling trend
- The observed Eurasian winter cooling trend over 1998–2012 arises from internal variability
- The dramatic change in Arctic sea ice enhances the Eurasian winter climate variability

Supporting Information:
- Sections S1 and S2, Figures S1–S5, and Tables S1–S3

Correspondence to:
C. Li,
chao.li@mpimet.mpg.de

Citation:
Li, C., B. Stevens, and J. Marotzke (2015), Eurasian winter cooling in the warming hiatus of 1998–2012, *Geophys. Res. Lett.*, *42*, 8131–8139, doi:10.1002/2015GL065327.

Received 10 JUL 2015
Accepted 9 SEP 2015
Accepted article online 12 SEP 2015
Published online 3 OCT 2015

Eurasian winter cooling in the warming hiatus of 1998–2012

Chao Li[1,2,3], Bjorn Stevens[2], and Jochem Marotzke[2]

[1]Cluster of Excellence CliSAP, University of Hamburg, Hamburg, Germany, [2]Max Planck Institute for Meteorology, Hamburg, Germany, [3]Research Unit Sustainability and Global Change, University of Hamburg, Hamburg, Germany

Abstract We investigate the relative magnitudes of the contributions of surface temperature trends from different latitude bands to the recent warming hiatus. We confirm from five different global data sets that the global-mean surface temperature trend in the period 1998–2012 is strongly influenced by a pronounced Eurasian winter cooling trend. To understand the drivers of this winter cooling trend, we perform three 20-member ensembles of simulations with different prescribed sea surface temperature and sea ice in the atmospheric model ECHAM6. Our experimental results suggest that the Arctic sea ice loss does not drive systematic changes in the Northern Hemisphere large-scale circulation in the past decades. The observed Eurasian winter cooling trend over 1998–2012 arises essentially from atmospheric internal variability and constitutes an extreme climate event. However, the observed reduction in Arctic sea ice enhances the variability of Eurasian winter climate and thus increases the probability of an extreme Eurasian winter cooling trend.

1. Introduction

Global-mean surface temperature (GMST) has shown a comparatively small warming trend over 1998–2012, termed a hiatus [*Meehl et al.*, 2011; *Flato et al.*, 2013; *Kosaka and Xie*, 2013]. The relative magnitudes and the underlying mechanisms of the regional contributions to the hiatus are not well understood. Here we investigate the contributions of observed surface temperature trends within different latitude bands, and we explore the cause of Northern Hemisphere (NH) midlatitude winter cooling using large ensembles of sensitivity simulations with an atmospheric general circulation model (AGCM).

Two major schools of thought have been developed that try to explain the causes of the recent surface warming hiatus as either external or internal: on the one hand, decreasing radiative forcing due to an increase of stratospheric aerosol [*Solomon et al.*, 2011; *Santer et al.*, 2014], or a more pronounced solar minimum through 2009 [*Kaufmann et al.*, 2011]; and on the other hand, internal climate variability manifest primarily as tropical-Pacific decadal variability [*Meehl et al.*, 2013; *Kosaka and Xie*, 2013; *Trenberth and Fasullo*, 2013; *Trenberth et al.*, 2014; *Dai et al.*, 2015], in turn associated with enhanced ocean heat uptake due to the intensification of the wind-driven circulation [*Meehl et al.*, 2011; *Katsman and van Oldenborgh*, 2011; *Meehl et al.*, 2013; *Watanabe et al.*, 2013; *Balmaseda et al.*, 2013; *England et al.*, 2014]. By analyzing 15 year trends of GMST in Coupled Model Intercomparison Project Phase 5 (CMIP5) simulations and observations, *Marotzke and Forster* [2015] demonstrated the generally dominant role of internal variability in shaping 15 year GMST trends in comprehensive models. Although many studies support the conclusion that the recent warming hiatus is a manifestation of internal variability, the different regional contributions to surface temperature trend, and their origin, are still under debate. In contrast to the tropical-Pacific dominated view, *Chen and Tung* [2014] suggested that the recent warming hiatus is mainly caused by heat transport to greater depth in the Atlantic and the Southern Oceans. *Cohen et al.* [2012a] suggested that the warming hiatus in recent decades is a seasonal phenomenon that is largely associated with anomalously cold NH winter land surface temperatures. By restoring observed sea surface temperature (SST) anomalies over the tropical eastern Pacific in a coupled climate model, *Kosaka and Xie* [2013] reproduced the GMST trend but not the winter trend over Eurasia. This suggests that mechanisms other than cooling in the tropical Pacific might also contribute to the warming hiatus.

Severe cold-weather events have occurred frequently across Eurasia and the United States and are often associated with a negative phase of the Arctic Oscillation (AO) [*Cohen et al.*, 2010; *Blunden et al.*, 2011; *Overland et al.*, 2011; *Liu et al.*, 2012; *Zhang et al.*, 2012] and an increase in high-latitude moisture and in Eurasian autumn

snow cover [*Cohen et al.*, 2012b]. Previous observational studies showed a statistically significant relationship between cold surface temperature anomalies over Eurasia and warm Arctic surface temperature anomalies owing to the rapid loss of Arctic sea ice [*Overland et al.*, 2011; *Liu et al.*, 2012; *Francis and Vavrus*, 2012; *Cohen et al.*, 2012b, 2013, 2014]. In AGCM sensitivity experiments with sea ice removed from the Barents-Kara Sea, *Petoukhov and Semenov* [2010] found a strong continental-scale winter cooling, but *Gerber et al.* [2014] found that the imposed sea ice anomalies only weakly affect Eurasian winter mean temperature. *Kim et al.* [2014] found that decreased Arctic sea ice during early winter led to a weakened polar vortex, thus inducing a negative AO and a negative anomaly in midlatitude surface temperature in winter. However, with a similar experimental setup as *Kim et al.* [2014], *Mori et al.* [2014] found no systematic response of the AO to Arctic sea ice decline; nonetheless, sea ice decline led to more frequent Eurasian blocking situations associated with changes in the regional atmospheric circulation over Eurasia, favoring cold-air advection to Eurasia and hence, severe winters. Arctic sea ice loss over interannual time scales has thus previously been shown to influence Eurasian winter temperatures, but whether such an influence exists for the present hiatus period and the degree of its influence remains unclear.

Here we investigate the contribution of the NH midlatitude winter cooling trend to the GMST trend. We also perform three sorts of sensitivity experiments with an AGCM to understand whether mechanisms can be identified to help explain the present hiatus.

2. Data and Methods

2.1. Observations

We use three observational surface temperature data sets, from the Met Office Hadley Centre and Climatic Research Unit (HadCRUT4) [*Morice et al.*, 2012], the NASA Goddard Institute for Space Studies (GISTEMP) [*Hansen et al.*, 2010], and the NOAA Merged Land-Ocean Surface Temperature Analysis (MLOST) [*Smith et al.*, 2008]. We calculate the surface temperature linear trend with an ordinary least squares fit. To evaluate whether the recent warming hiatus is largely influenced by coverage bias in observational records due to missing Arctic warming (as suggested by *Cowtan and Way* [2014]), we also use two reanalysis data sets, one from the European Centre for Medium-Range Weather Forecasts (ERA-interim) [*Dee et al.*, 2011] and one from the National Centers for Environmental Prediction-Department of Energy (NCEP-DOE) Reanalysis 2 [*Kanamitsu et al.*, 2002]. We create the zonal-mean and global-mean surface temperature trend by area-weighted averaging in the various latitude bands. In contrast to the two reanalysis data sets, the observed surface temperature data sets contain missing values in some grid boxes. When calculating the surface temperature trend with the three observational data sets, we give zero weight to grid boxes without data and do not apply interpolation to fill the data gaps in these grid boxes.

We explore how NH regional temperature trends are related to the NH atmospheric circulations. To this end, we construct the DJF (December-January-February) AO index and Pacific-North American Pattern (PNA) index by projecting the monthly mean sea level pressure (SLP) anomalies from ERA-interim and NCEP-DOE data poleward of 20°N onto the leading patterns of the AO and PNA. We use daily mean 500 hPa geopotential height from ERA-interim and NCEP-DOE data to calculate NH DJF blocking frequency (percentage of time with blocking) with the method of *Lejenäs and Økland* [1983] as modified by *Tibaldi and Molteni* [1990]. A blocking event is recognized when the meridional gradient of geopotential height at 500 hPa reverses and persists for 5 days between 40°N and 80°N. To be consistent with the ERA-Interim data, we interpolate the NCEP-DOE daily 500 hPa geopotential height from its original horizontal grid of 2.5°×2.5° to a finer 1.5°×1.5° grid to calculate the NH blocking frequency.

2.2. Model and Experimental Design

We perform a series of numerical experiments with prescribed SST and Arctic sea ice distribution in the period of 1979–2012 by using the AGCM ECHAM6 with a horizontal resolution of T63 (approximately 1.875° on a Gaussian grid) and 47 vertical levels extending to 0.01 hPa [*Stevens et al.*, 2013]. The model is coupled to a submodel for land and vegetation, JSBACH [*Reick et al.*, 2013]. Similarly to the CMIP5 historical experiments in the period of 1979–2005 [*Giorgetta et al.*, 2013], we use natural forcing (Earth orbit, solar irradiance, natural tropospheric aerosols, and stratospheric aerosols from volcanic eruptions), and anthropogenic forcing (five well-mixed greenhouse gases, anthropogenic aerosols, and land use). The stratospheric aerosols from volcanic eruptions decay toward zero after year 1999. For the years 2005–2012, we apply the forcing prescribed by the RCP4.5 scenario. For the oceanic boundary conditions in the period of 1979–2012, we use SST and sea

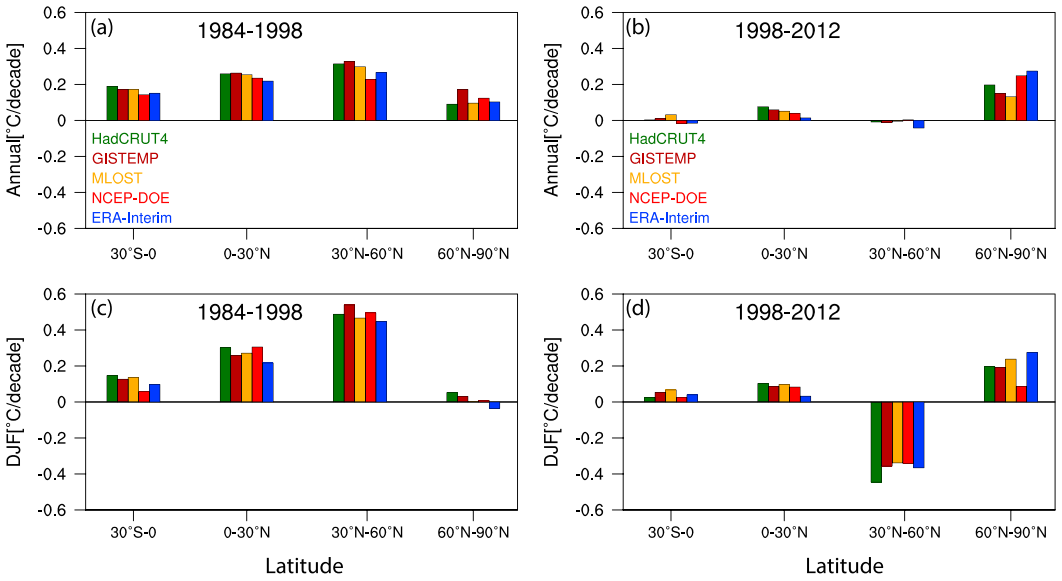

Figure 1. Scaled observed zonal-mean surface temperature trend at different latitude bands. (a) and (b) for annual mean, (c) and (d) for DJF, Figures 1a and 1c for the period of 1984–1998, (Figures 1b and 1d for the period of 1998–2012. The different latitude bands can be directly compared for their influence on the global mean because the trends are scaled by area. No interpolation was done to fill the data gaps in the three observational data sets HadCRUT4, GISTEMP, and MLOST.

ice boundary condition data sets as supplied by the Program for Climate Model Diagnosis and Intercomparison (PCMDI). Because January and February 2013 are not included in this data set, our simulations end in December 2012, and we evaluate simulated DJF trends over the 14 year period 1998–2011 for the last period considered here.

We conduct three sets of Atmospheric Model Intercomparison Project (AMIP)-type experiments: in the first set, the atmospheric model is subject to boundary conditions of observed SST and sea ice distributions over 1979–2012 (AMIP); in the second set, the impact of Arctic sea ice changes is excluded by taking SST and sea ice concentration as the climatological annual cycle over 1979–2012 north of 60°N (ACLI); and in the third set, SST and sea ice concentration are taken as the climatological annual cycle over 1979–2012 everywhere (GCLI). For each set, an ensemble of 20 simulations is performed—comprising a total of 60 experiments. The GCLI experiments exclude the forced response of the atmospheric circulation to ocean variations and represent the purely atmospheric internal variability together with the direct response to natural and anthropogenic forcing. To calculate the NH winter blocking frequency, from model output the daily 500 hPa geopotential height is interpolated from the original model grid to a 1.5° × 1.5° grid, to be consistent with ERA-Interim.

3. Results

3.1. Observational Evidence

Our analyses show that the GMST trend over 1998–2012 is much smaller than that over 1984–1998 in all data sets (Table S1 in the supporting information). Consistent with the three observational data sets (despite their missing Arctic warming), a large reduction of GMST trend over 1998–2012 is also apparent in both the ERA-interim and NCEP-DOE products, which include a large warming trend over the Arctic. This suggests that the warming hiatus over 1998–2012 is a robust phenomenon, although the warming trend over 1998–2012 might be underestimated owing to incomplete observational coverage as suggested by *Cowtan and Way* [2014] or by ocean data biases as suggested by *Karl et al.* [2015]. Instead, we confirm with five different global data sets that the GMST trend over 1998–2012 is reduced by 59% to 85% compared to the warming trend over 1984–1998 (Table S1 in the supporting information), supporting the notion of a recent surface-warming slowdown.

We examine the seasonality of the change in GMST trend by comparing the periods of 1998–2012 and 1984–1998 in all data sets. The reduction of the 15 year GMST trend over 1998–2012 happens in all seasons. However, we confirm that the largest reduction happens in boreal winter [*Cohen et al.*, 2012a] where the

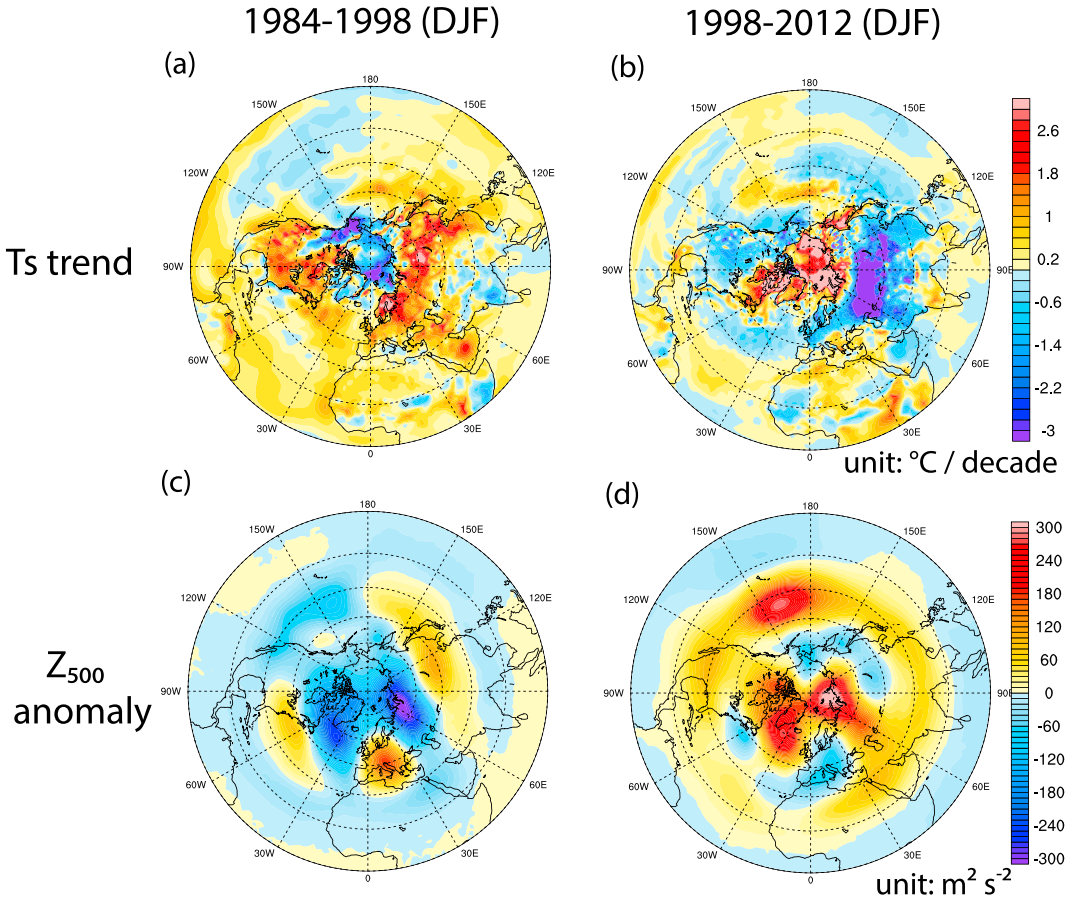

Figure 2. Observed DJF surface temperature trend in ERA-Interim over (a) 1984–1998 and (b) 1998–2012, and DJF 500 hPa geopotential height anomaly in ERA-Interim for the period of (c) 1984–1998 and (d) 1998–2012. The anomaly is relative to the DJF mean of 1979–2012.

trend reverses from a warming slightly larger than 0.2°C/decade in 1984–1998 to a cooling slightly greater in magnitude than 0.1°C/decade in 1998–2012 (Figure S1 in the supporting information). Over 1984–1998, an almost uniform warming of around 0.2°C/decade of GMST appears in all seasons (Figure S1). Over 1998–2012, the GMST in spring and summer shows a warming of about 0.1°C/decade, which is only half of the warming over 1984–1998 (Figure S1). The recent warming hiatus is thus not only a NH winter phenomenon, but the reduction of GMST trend in NH winter over 1998–2012 does play a disproportionate role.

To quantify the contribution to global temperature trend reduction from different latitude bands, we calculate the area-weighted scaled surface temperature trend in four different latitude bands: 30°S–0, 0–30°N, 30°N–60°N, 60°N–90°N (Figure 1). Compared to the trend over 1984–1998, the warming trend over 1998–2012 is reduced by about 0.2°C/decade equatorward of 30°; the largest temperature trend reduction of about 0.3°C/decade appears in the NH midlatitudes (Figures 1a and 1b). By contrast, the warming trend in the Arctic (60°N–90°N) is larger over 1998–2012 than over 1984–1998. The largest trend reduction happens mainly in the NH midlatitude winter where the surface temperature trend changes from a warming trend greater than 0.4°C/decade over 1984–1998 to a cooling trend beyond -0.4°C/decade over 1998–2012 (Figures 1c and 1d). The temperature trends in the latitude band south of 30°S are small, and the changes in temperature trends south of 30°S contribute little (Figure S2). The results are similar for a 14 year trend starting from 1999 and also a 13 year trend starting from 2000. In distinction to previous studies, which suggested that the recent warming hiatus is mainly caused by cooling in the tropical Pacific [*Meehl et al.*, 2013; *Kosaka and Xie*, 2013; *England et al.*, 2014], we find that the recent warming hiatus is a combination of a tropical trend reduction and a NH midlatitude trend reduction due to a strong NH winter cooling (Figure 1).

During the period of 1984–1998, large warming trends of DJF surface temperature occur over NH midlatitude continents (Figure 2a). The associated circulation anomalies in 500 hPa geopotential height appear similar to

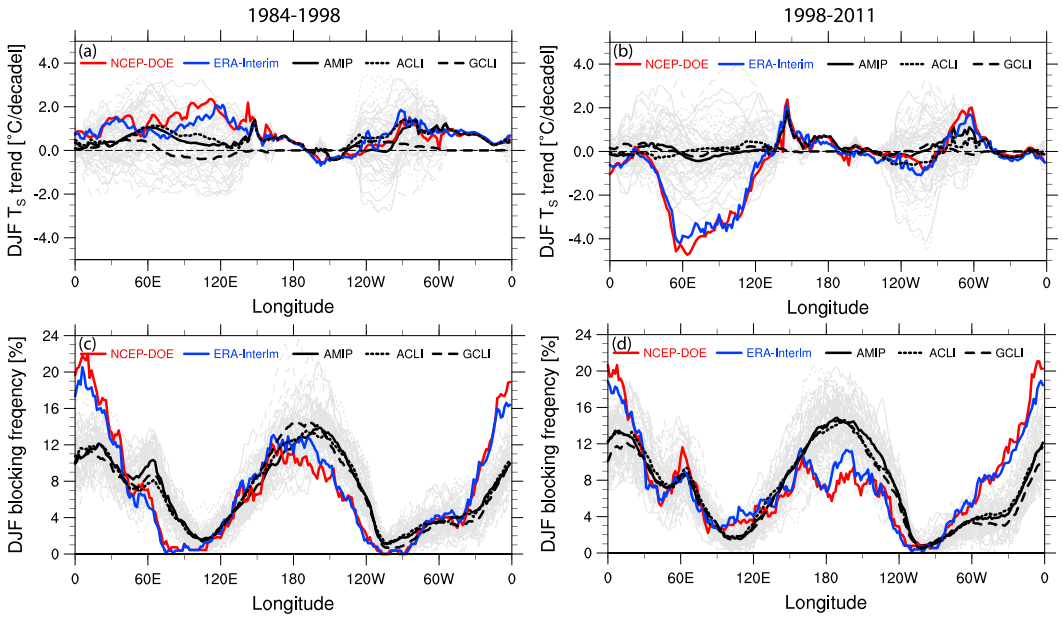

Figure 3. Observed and simulated DJF surface temperature trend from 40°N to 60°N over (a) 1984–1998 and (b) 1998–2011, and observed and simulated NH DJF blocking frequency over (c) 1984–1998 and (d) 1998–2011. ERA-interim and NCEP-DOE data are shown as solid blue and red lines, respectively, the AMIP ensemble is shown in solid black, the ACLI ensemble as black short-dashed lines, and the GCLI-ensemble as black long-dashed lines. The gray lines are from all simulated realizations.

a positive AO (Figure 2c). Additionally, less frequent winter blocking events in ERA-interim and NCEP-DOE over Eurasia (50°E–120°E) tend to bring less cold air from NH high latitudes to midlatitudes (Figure 3c). Over 1998–2012, the spatial pattern of surface temperature trends exhibits a warming Arctic-cooling NH continent pattern, with a strong warming trend of up to 3°C/decade over the Arctic and a cooling trend of up to 4°C/decade over Eurasia (Figure 2b). The associated circulation anomalies in 500 hPa geopotential height appear similar to a negative AO (Figure 2d), and more frequent winter blocking events in ERA-interim and NCEP-DOE over Eurasia (50°E–120°E) tend to bring more cold air from NH high latitudes to midlatitudes (Figure 3d). The observed change in NH high-latitude atmospheric circulation thus favors the observed NH midlatitude surface temperature trends over 1998–2012. In the following, we explore quantitatively the connection between NH circulation, NH temperature trend, and Arctic sea ice loss over the past decades.

3.2. Large-Scale Atmospheric Circulation Change

We first examine whether Arctic sea ice loss drives systematic changes in NH large-scale atmospheric circulation as measured by systematic changes in the AO and PNA, through the three sets of numerical experiments AMIP, ACLI, and GCLI. We extract the dominant modes of NH atmospheric circulation by applying empirical orthogonal function (EOF) analysis to the DJF mean SLP anomalies poleward of 20°N to the reanalysis data and model output. The first two leading modes explain about half or more of the NH large-scale atmospheric circulation variance and are interpreted as the AO and PNA (Figures S3 and S4).

A statistically significant correlation between the ERA-interim and the model-simulated ensemble mean AO and PNA indices in both AMIP and ACLI suggests that when forced by observed SSTs, ECHAM6 can reasonably simulate the variations of NH large-scale atmospheric circulation over 1979–2012 (Tables S2 and S3 in the supporting information). The AO index of the ACLI ensemble mean is highly correlated with that of AMIP, with a correlation coefficient of 0.87 (statistically significant at the 0.01 level, student's t-test), and the PNA index of the ACLI ensemble mean is also highly correlated with that of AMIP, with a correlation coefficient of 0.58 (statistically significant at the 0.01 level, Student's *t* test). These high correlation coefficients suggest that the Arctic sea ice changes do not drive systematic changes of NH large-scale atmospheric circulations in the past decades.

3.3. Eurasian Winter Temperature Change and Winter Blocking Frequency

We now examine the potential connection between the observed changes in Eurasian winter surface temperature trend, regional atmospheric circulation change, and the rapid Arctic sea ice loss, again using the

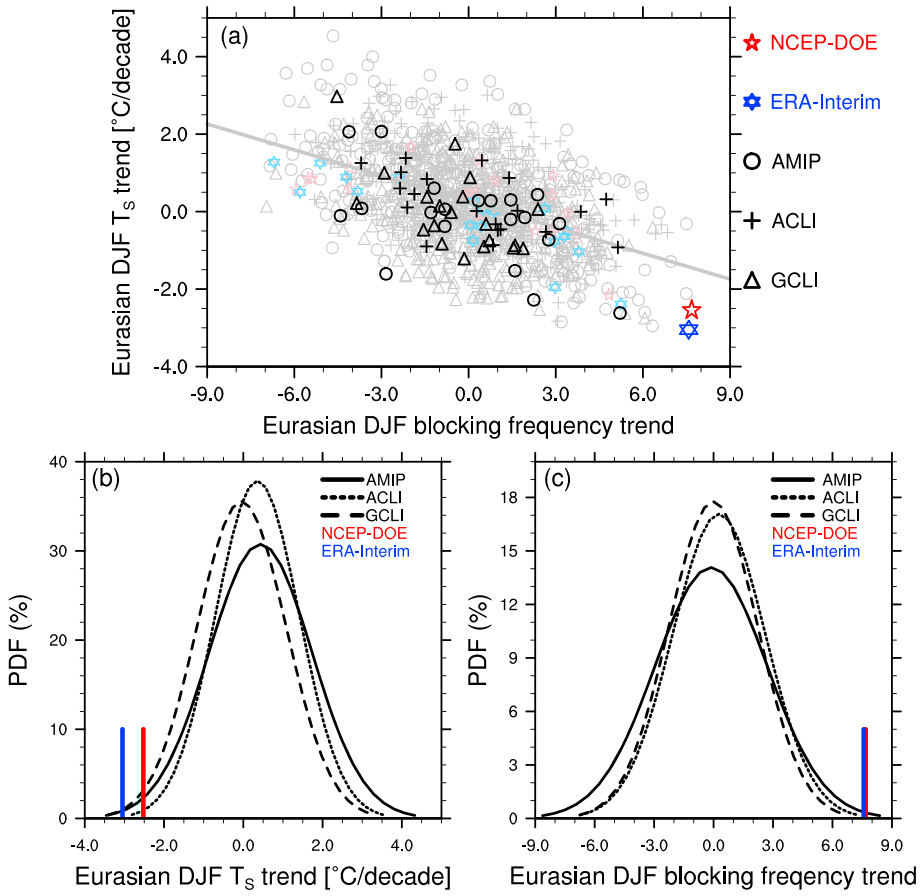

Figure 4. (a) Observed and simulated 15 year trends in Eurasian DJF surface temperature against the 15 year trends in Eurasian DJF blocking frequency in the period of 1979–2012. Trends over 1998–2011 are shown in blue (ERA-interim), red (NCEP-DOE), and black (simulations); 15 year trends over all other periods are shown in light blue (ERA-interim), light red (NCEP-DOE) and gray (simulations). The gray line represents a linear regression of all simulated 15 year trends. (b) Smoothed normalized distribution of all simulated 15 year trends of Eurasian DJF surface temperature as shown in Figure 4a. The observed 15 year trend over 1998–2011 is shown in blue (ERA-interim) and red (NCEP-DOE). (c) As in Figure 4b, but for 15 year trends in Eurasian DJF blocking frequency. The Eurasian DJF surface temperature trend is calculated in the domain 60°E–120°E, 40°N–60°N, and the Eurasian DJF blocking frequency is calculated in the domain 50°E–120°E.

sensitivity experiments AMIP, ACLI, and GCLI. Over 1984–1998, the ensemble mean Eurasian winter surface temperature in AMIP and ACLI shows a weaker warming trend than in the reanalysis data, with a maximum of about 1°C/decade (50°E–120°E in Figure 3a). Over 1998–2011, no ensemble mean simulated Eurasian winter surface temperature shows a cooling trend. Furthermore, none of the ensemble members shows a cooling trend as strong as observed. The four simulations with pronounced Eurasian winter cooling trend larger than −2°C/decade all come from AMIP simulations (50°E–120°E in Figure 3b). Our simulations thus provide no support for the suggestion that the changes in Arctic sea ice and high-latitude SST drive a systematic cooling trend of Eurasian winter temperature in the hiatus period. However, the observed high-latitude changes in SST and sea ice lead to greater variance in the 15 year trend of Eurasian winter surface temperature (see below), so that some ensemble members reproduce the observed area-averaged winter cooling during the recent hiatus.

We do not find systematic differences in Eurasian winter blocking frequency between simulations with or without Arctic sea ice and SST changes (50°E–120°E in Figures 3c and 3d). As most other climate models, ECHAM6 underestimates the atmospheric blocking frequency in the Atlantic sector (0°E–50°E in Figures 3c and 3d), and it has been argued that the underestimation of winter blocking frequency is mainly caused by insufficient horizontal resolution [*Matsueda et al.*, 2009]. Here we focus on the winter blocking frequency over Eurasia, where ECHAM6 shows less of a systematic error in winter blocking frequency. In the reanalyses,

a Eurasian winter blocking pattern occurs more frequently in 1998–2011 than in 1984–1998, but for both periods Eurasian winter blocking frequencies are largely in the range of the simulated ensemble spread. The changes in Eurasian winter blocking frequency thus appear largely to be a manifestation of atmospheric internal variability and not a response to changes in Arctic sea ice and high-latitude SST in the past decades—a notion that we now make more quantitative.

In the two reanalysis data sets, the 15 year Eurasian winter cooling trend over 1998–2012 is more pronounced than any 15 year trend with start years between 1979 and 1997 (Figure 4a). And considering the simulated frequency of 15 year Eurasian winter temperature in our 60-member ensemble, fewer than 5% of the simulated 15 year trends of the Eurasian DJF temperature lie in the tail relative to the observed trend over 1998–2011 (Figure 4b). Furthermore, fewer than 5% of the simulated 15 year trends of the Eurasian DJF blocking frequency show a similar increase in DJF blocking frequency trend as the observations (Figure 4c). Hence, the strong cooling trend of Eurasian DJF temperature over 1998–2012 is still in the range of the internal variability, but this cooling indicates an extreme climate event.

The average of 15 year Eurasian winter temperature trends in AMIP is about 0.43°C/decade, which is slightly higher than in ACLI (0.35°C/decade). The variance ratio of Eurasian winter temperature trends between AMIP and ACLI is 1.53, and the variance ratio of Eurasian winter temperature trends between AMIP and GCLI is 1.34. With a nonparametric test with a moving blocks bootstrap [*Wilks*, 1997] (details in section S2 of the supporting Information), the variation of Eurasian winter temperature trends in AMIP is significantly larger than that in ACLI and GCLI , but the variation of Eurasian winter temperature trends in ACLI is not significantly different from that in GCLI (Figure S5a). Similar to the Eurasian winter temperature trend, the variation of Eurasian winter blocking trends in AMIP is significantly larger than that in ACLI and GCLI, but the variation of Eurasian winter blocking trends in ACLI is not significantly different from that in GCLI (Figure S5b). Our sensitivity experiments show no discernible shift in the ensemble mean of Eurasian winter temperature trends and the Eurasian blocking frequency associated with sea ice changes in the period 1998–2011 (Figure 4). At least in our model it is thus difficult to maintain that the loss of Arctic sea ice and the associated increase of high-latitude SST drive systematic changes in the Eurasian climate in the last decades. Our simulations do provide some evidence that changes in Arctic sea ice and high-latitude SST could slightly enhance the variability of the Eurasian winter climate and thus increase the probability of otherwise unusually large cooling (or warming) trends (Figure 4).

4. Conclusion

We confirm from three observational and two reanalysis data sets that the GMST warming hiatus over 1998–2012 is strongly influenced by a pronounced NH midlatitude winter cooling trend, in addition to a reduction in warming trend over the NH tropics. Because this strong midlatitude winter cooling trend was not reproduced by restoring the observed SST over the tropical Pacific in a coupled climate model [*Kosaka and Xie*, 2013], we explore the impact of Arctic sea ice loss and the associated warming of high-latitude SST on the NH midlatitude winter climate in three sets of AMIP-type experiments. Our model shows no influence of Arctic sea ice loss and high-latitude SST increase on NH large-scale atmospheric circulation features such as AO, PNA, and the Eurasian winter blocking frequency in the past decades. The observed increase in Eurasian winter blocking frequency over 1998–2012 appears instead to be a manifestation of atmospheric internal variability. The observed Eurasian winter cooling trend over 1998–2012 is unprecedented among 15 year trends since 1979 and lies within the 5% tail of the ensemble of simulated temperature trends, marking the observed cooling over 1998–2012 as an extreme climate event. Our simulations do not support a suggestion that the loss of Arctic sea ice together with the high-latitude SST increase drive a systematic cooling trend of Eurasian winter climate, but the observed reduction in Arctic sea ice associated with high-latitude warming could enhance the variability of Eurasian winter climate and thus increases the probability of the Eurasian winter reaching the extreme cold trend of the recent hiatus period.

Acknowledgments

We acknowledge the Met Office Hadley Centre, the NASA Goddard Institute for Space Studies, and the NOAA National Climatic Data Center for making the observed global surface temperature data available, and the European Centre for Medium-Range Weather Forecasts and the NOAA National Climatic Data Center for the atmospheric reanalysis data. We thank the PCMDI for providing the AMIP boundary conditions of SST and sea ice concentration. More details on AMIP SST and sea ice concentration are available on the PCMDI website (http://www-pcmdi.llnl.gov/projects/amip/). We thank Johann Jungclaus and Dirk Notz for helpful discussions and Dirk Notz and Christopher Hedemann for comments on the manuscript. We thank Monika Esch and Karl-Hermann Wieners for their assistance in setting up the AMIP simulations. The model simulations were carried out on the supercomputing system of the German Climate Computing Center (DKRZ) in Hamburg, Germany.

The Editor thanks Judah Cohen and an anonymous reviewer for their assistance in evaluating this paper.

References

Balmaseda, M. A., K. E. Trenberth, and E. Källén (2013), Distinctive climate signals in reanalysis of global ocean heat content, *Geophys. Res. Lett.*, *40*, 1754–1759, doi:10.1002/grl.50382.

Blunden, J., D. S. Arndt, and M. O. Baringer (2011), State of the climate in 2010, *Bull. Amer. Meteor. Soc.*, *92*, S1–S236, doi:10.1175/1520-0477-92.6.S1.

Chen, X., and K.-K. Tung (2014), Varying planetary heat sink led to global-warming slowdown and acceleration, *Science*, *345*, 897–903, doi:10.1126/science.1254937.

Cohen, J., J. Foster, M. Barlow, K. Saito, and J. Jones (2010), Winter 2009/10: A case study of an extreme Arctic Oscillation event, *Geophys. Res. Lett.*, *37*, L17707, doi:10.1029/2010GL044256.
Cohen, J., J. Furtado, M. Barlow, V. Alexeev, and J. Cherry (2012a), Asymmetric seasonal temperature trends, *Geophys. Res. Lett.*, *39*, L04705, doi:10.1029/2011GL050582.
Cohen, J., J. Furtado, J. M. Barlow, V. Alexeev, and J. Cherry (2012b), Arctic warming, increasing fall snow cover and widespread boreal winter cooling, *Environ. Res. Lett.*, *7*, 11004, doi:10.1088/1748-9326/7/1/014007.
Cohen, J., J. Jones, J. C. Furtado, and E. Tziperman (2013), Warm Arctic, cold continents: A common pattern related to Arctic sea ice melt, snow advance, and extreme winter weather, *Oceanography*, *26*(4), 150–160.
Cohen, J., et al. (2014), Recent Arctic amplification and extreme mid-latitude weather, *Nat. Geosci.*, *7*, 627–637.
Cowtan, K., and R. G. Way (2014), Coverage bias in the HadCRUT4 temperature series and its impact on recent temperature trends, *Q. J. R. Meteorol. Soc.*, *140*, 1935–1944, doi:10.1002/qj.2297.
Dai, A., J. C. Fyfe, S. P. Xie, and X. Dai (2015), Decadal modulation of global surface temperature by internal climate variability, *Nat. Clim. Change*, *5*, 555–559, doi:10.1038/nclimate2605.
Dee, D. P., et al. (2011), The ERA-Interim reanalysis: Configuration and performance of the data assimilation system, *Q. J. R. Meteorol. Soc.*, *137*, 553–597.
England, M. H., et al. (2014), Intensified Pacific Ocean wind-driven circulation during the ongoing warming hiatus, *Nat. Clim. Change*, *4*, 222–227.
Flato, G. et al. (2013), *Climate Change 2013: The Physical Science Basis. Contribution of Working Group I to the Fifth Assessment Report of the Intergovernmental Panel on Climate Change*, edited by T. F. Stocker et al., pp. 741–866, Cambridge Univ. Press, Cambridge, U. K., and New York.
Francis, J. A., and S. J. Vavrus (2012), Evidence linking Arctic amplification to extreme weather in mid-latitudes, *Geophys. Res. Lett.*, *39*, L06801, doi:10.1029/2012GL051000.
Gerber, F., J. Sedláček, and R. Knutti (2014), Influence of the western North Atlantic and the Barents Sea on European winter climate, *Geophys. Res. Lett.*, *41*, 561–567, doi:10.1002/2013GL058778.
Giorgetta, M. A., et al. (2013), Climate and carbon cycle changes from 1850 to 2100 in MPI-ESM simulations for the Coupled Model Intercomparison Project phase 5, *J. Adv. Model. Earth Syst.*, *5*, 572–597, doi:10.1002/jame.20038.
Hansen, J., R. Ruedy, M. Sato, and K. Lo (2010), Global surface temperature change, *Rev. Geophys.*, *48*, RG4004, doi:10.1029/2010RG000345.
Karl, T. R., et al. (2015), Possible artifacts of data biases in the recent global surface warming hiatus, *Science*, *348*, 1469–1472, doi:10.1126/science.aaa5632.
Katsman, C. A., and G. J. van Oldenborgh (2011), Tracing the upper ocean's "missing heat", *Geophys. Res. Lett.*, *38*, L14610, doi:10.1029/2011GL048417.
Kaufmann, R. F., H. Kauppi, M. L. Mann, and J. H. Stock (2011), Reconciling anthropogenic climate change with observed temperature 1998-2008, *Proc. Natl. Acad. Sci. U.S.A.*, *108*(29), 11,790–11,793, doi:10.1073/pnas.1102467108.
Kanamitsu, M., W. Ebisuzaki, J. Woollen, S-K Yang, J. J. Hnilo, M. Fiorino, and G. L. Potter (2002), NCEP-DOE AMIP-II Reanalysis (R-2), *Bull. Am. Meteorol. Soc.*, *83*, 1631–1643.
Kim, B. M., S. W. Son, S. K. Min, J. H. Jeong, S. J. Kim, X. D. Zhang, T. Shim, and J. H. Yoon (2014), Weakening of the stratospheric polar vortex by Arctic sea-ice loss, *Nat. Commun.*, *5*, 4646, doi:10.1038/ncomms5646.
Kosaka, Y., and S. P. Xie (2013), Recent global-warming hiatus tied to equatorial Pacific surface cooling, *Nature*, *501*(7467), 403–407.
Lejenäs, H., and H. Økland (1983), Characteristics of northern hemisphere blocking as determined from a long time series of observational data, *Tellus*, *35A*, 350–362.
Liu, J., J. A. Curry, H. Wang, M. Song, and R. M. Horton (2012), Impact of declining Arctic sea ice on winter snowfall, *Proc. Natl. Acad. Sci. U.S.A.*, *109*, 4074–4079, doi:10.1073/pnas.1114910109.
Marotzke, J., and P. M. Forster (2015), Forcing, feedback and internal variability in global temperature trends, *Nature*, *517*, 565–570, doi:10.1038/nature14117.
Matsueda, M., R. Mizuta, and S. Kusunoki (2009), Future change in wintertime atmospheric blocking simulated using a 20-km mesh atmospheric global circulation model, *J. Geophys. Res.*, *114*, D12114, doi:10.1029/2009JD011919.
Meehl, G. A., J. M. Arblaster, J. T. Fasullo, A. Hu, and K. E. Trenberth (2011), Model-based evidence of deep-ocean heat uptake during surface-temperature hiatus periods, *Nat. Clim. Change*, *1*, 360–364.
Meehl, G., A. Hu, J. Arblaster, J. Fasullo, and K. E. Trenberth (2013), Externally forced and internally generated decadal climate variability associated with the Interdecadal Pacific Oscillation, *J. Clim.*, *26*, 7298–7310.
Mori, M., M. Watanabe, H. Shiogama, J. Inoue, and M. Kimoto (2014), Robust Arctic sea-ice influence on the frequent Eurasian cold winters in past decades, *Nat. Geosci.*, *7*, 869–873, doi:10.1038/ngeo2277.
Morice, C., J. Kennedy, N. Rayner, and P. Jones (2012), Quantifying uncertainties in global and regional temperature change using an ensemble of observational estimates: The HadCRUT4 dataset, *J. Geophys. Res.*, D08101, doi:10.1029/2011JD017187.
Overland, J. E., K. R. Wood, and M. Wang (2011), Warm Arctic—Cold continents: Climate impacts of the newly open Arctic sea, *Polar Res.*, *30*, 15,787, doi:10.3402/polar.v30i0.15787.
Petoukhov, V., and V. A. Semenov (2010), A link between reduced Barents-Kara sea ice and cold winter extremes over northern continents, *J. Geophys. Res.*, *115*, D21111, doi:10.1029/2009JD013568.
Reick, C., T. Raddatz, V. Brovkin, and V. Gayler (2013), Representation of natural and anthropogenic land cover change in MPI-ESM, *J. Adv. Model. Earth Syst.*, *5*, 459–482, doi:10.1002/jame.20022.
Santer, B. D., et al. (2014), Volcanic contribution to decadal changes in tropospheric temperature, *Nat. Geosci.*, *7*, 185–189.
Smith, T. M., et al. (2008), Improvements to NOAA's historical merged land-ocean surface temperature analysis (1880–2006), *J. Clim.*, *21*, 2283–2293.
Solomon, S., et al. (2011), The persistently variable "background" stratospheric aerosol layer and global climate change, *Science*, *333*, 866–870, doi:10.1126/science.1206027.
Stevens, B., et al. (2013), Atmospheric component of the MPI-M Earth System Model: ECHAM6, *J. Adv. Model. Earth Syst.*, *5*, 146–172, doi:10.1002/jame.20015.
Tibaldi, S., and F. Molteni (1990), On the operational predictability of blocking, *Tellus*, *42A*, 343–365.
Trenberth, K. E., and J. T. Fasullo (2013), An apparent hiatus in global warming?, *Earth's Future*, *1*, 19–32.
Trenberth, K. E., J. T. Fasullo, G. Branstator, and A. S. Phillips (2014), Seasonal aspects of the recent pause in surface warming, *Nat. Clim. Change*, *4*, 911–916, doi:10.1038/nclimate2341.

Watanabe, M., Y. Kamae, M. Yoshimori, A. Oka, M. Sato, M. Ishii, T. Mochizuki, and M. Kimoto (2013), Strengthening of ocean heat uptake efficiency associated with the recent climate hiatus, *Geophys. Res. Let.*, *40*, 3175–3179, doi:10.1002/grl.50541.

Wilks, D. S. (1997), Resampling hypothesis tests for autocorrelated fields, *J. Clim.*, *10*, 65–82.

Zhang, X., C. Lu, and Z. Guan (2012), Weakened cyclones, intensified anticyclones and recent extreme cold winter weather events in Eurasia, *Environ. Res. Lett.*, *7*, 44015, doi:10.1088/1748-9326/8/4/044015.